

red clay), with occasional turbidites of sand; most contain a few foraminifers and coccoliths of Pleistocene or Recent age. Their lithology establishes the Recent and Pleistocene sedimentary regime in this area and is further evidence that the Cretaceous cores came from a unique outcrop.

To our knowledge this is the first report of Cretaceous red clays that are definitely deep-sea in origin, a fact of particular importance in the history of the Atlantic. Results of emission spectrochemical analysis suggest that deep oceanic clay can be distinguished from normal shales on the basis of the manganese content (2). Normal shales contain 300 to 850 ppm Mn whereas oceanic clays contain 4000 to 9180 ppm. A sample of red clay from a depth of 790 cm in core V 21-241 contains 5500 ppm Mn, a content similar to that of deep clays under the modern oceans (3). Presence of the red clay in the Cretaceous cores indicates that sediments were deposited below the carbonate compensation depth and suggests that the Cretaceous sea in this part of the Atlantic was at least as deep as at present.

We should also point out that, according to an interpretation of the seismic-profile records, the area of the horizon A outcrop was uplifted to its present depth (1). Thus it is possible that the depth of the water at the time of deposition of horizon A was greater than at present. Those who believe that the Atlantic Ocean basin is a geologically young feature must consider this point.

The exposure of abyssal Cretaceous sediments here must be partly attributed to erosion (1); the mixed faunas reported in several cores are additional evidence of this. The abundance of turbidites in the Cretaceous deposits reinforces the earlier suggestion that these beds were level, or nearly so, when deposited, so that major irregularities in the topography of horizon A probably result from postdepositional deformation. The exposure of horizon β appears to be more closely associated with regional uplift.

The presence of iron sulfide and the odor of hydrogen sulfide in core V 22-8 may demonstrate anaerobic conditions near the sediment-water interface in Cenomanian time at this site. Such conditions in younger sediments have been attributed to either ponding of stagnant bottom water by a topographic barrier (4) or depletion of oxygen by overabundance of organic sub-

stance (5). However, Emery (6) has pointed out that both hydrogen sulfide and iron sulfide can form in sediments beneath aerobic waters, but that the interstitial waters, because of their slow circulation, can become anaerobic. At present, the few seismic-profile records from this area show some evidence of sediment ponding during Cenomanian time.

TSUNEMASA SAITO
LLOYD H. BURCKLE
MAURICE EWING

Lamont Geological Observatory,
Columbia University,
Palisades, New York

References and Notes

1. J. I. Ewing, J. L. Worzel, M. Ewing, C. Windisch, *Science*, this issue.
2. S. K. el Wakeel and J. P. Riley, *Geochim. Cosmochim. Acta* **25**, 110 (1961); K. M. Horn and J. A. S. Adams, *ibid.* **30**, 279 (1966).
3. A chemical, mineralogic, and petrographic study of the sample was made by H. M. Dahl and W. L. Hall at Bellaire Research Laboratories of Texaco, Inc.
4. R. H. Fleming and R. Revelle, in *Recent Marine Sediments*, P. D. Trask, Ed. (Soc. Econ. Paleontologists Mineralogists Spec. Publ. **4**, 1955), p. 96.
5. K. M. Ström, *ibid.*, p. 356.
6. K. O. Emery, in *Habitat of Oil*, L. G. Weeks, Ed. (Amer. Assoc. Petroleum Geologists, Tulsa, Okla., 1958), p. 965.
7. Supported by ONR contract Nonr 266 (48) and NSF grant GA 558. We are greatly indebted to F. D. Bode, H. M. Dahl, and W. L. Hall of Bellaire Research Laboratories of Texaco, Inc. We also thank J. I. Ewing, C. Windisch, and X. Le Pichon for reviewing and discussing the manuscript. Figure 1 was drawn by P. Buhl. Lamont Geological Observatory contribution No. 997.

17 August 1966

Melting of Tin Telluride at High Pressures

Abstract. *The melting curve of tin telluride ($\text{Sn}_{0.496}\text{Te}_{0.504}$) was determined by differential thermal analysis at pressures between 5 and 40 kilobars. Near $844^\circ \pm 4^\circ\text{C}$ and 12.0 ± 1.0 kb, the liquid and two solid polymorphs coexist.*

The compounds of elements of groups IV and VI, GeS, GeSe, GeTe, SnS, SnSe, SnTe, PbS, PbSe, PbTe, a technologically interesting group of materials, are chemically and structurally related to each other and to the group V elements P, As, Sb, Bi. Recent high-pressure investigations (1) have suggested further simple and useful correlations for phase relations of chemically and structurally related groups of elements and compounds. We now report determination of the melting curve of SnTe at pressures up to 40 kb; we have correlated some of

the data for phase relations of the group IV-group VI compounds.

Differential thermal analysis techniques (2) in piston-cylinder apparatus were used to observe meltings and freezings at elevated pressures. Freshly powdered samples (3) of $\text{Sn}_{0.496}\text{Te}_{0.504}$, contained in tantalum (two runs) and molybdenum capsules sealed (4) with Pyrex, were run in previously described furnace assemblies (5). Chromel-alumel thermocouples, typically about 0.3 mm from the sample, measured temperature; we attempted no corrections for the effects of pressure on thermocouple emf.

Results for the melting of SnTe are shown in Fig. 1. Heating signals were taken for the phase boundary in the Mo and Ta (1st) runs; for the Ta (2nd) run, cooling signals were considerably more distinct than heating signals. The overall precision in temperature appears to be within about 3°C (Fig. 1), although precision and reproducibility in a given run were within about 1° or 2°C . Friction corrections (2) were made by averaging compression and decompression pressures for the same transition temperature, with typical "single-values" of friction being 1.9 kb near 20 kb and 2.5 kb near 40 kb. Overall accuracy for pressure appears to be within about 1.0 kb.

A liquid-solid-solid triple point occurs near $844^\circ \pm 4^\circ\text{C}$ and 12.0 ± 1.0 kb (Fig. 1). No temperature-induced solid-solid transitions are known at zero pressure for the BI (rocksalt) structure in SnTe, and no signals were observed in our high-temperature, high-pressure explorations within stability fields of the solid phases. The structure of the solid melting below 12 kb is therefore presumed to be BI; above 12 kb, the phase that melts is apparently that reported by Kafalas and Mariano (6) as being stable above 18 kb at room temperature. The solid-solid phase boundary, which we could not detect, is drawn from the triple point toward the room temperature 18 kb coordinate (dotted line in Fig. 1).

Near zero pressure, the $\text{Sn}_{0.496}\text{Te}_{0.504}$ compound melts congruently at $805.9^\circ \pm 0.3^\circ\text{C}$ (7). With increasing pressure, the melting possibly becomes incongruent; our experiments could not delineate any such effect but did suggest an upper limit of $\sim 5^\circ\text{C}$ to any range of incongruent melting below 40 kb. Difficulties (2) in obtaining data below ~ 5 kb preclude accurate determination of the initial melting

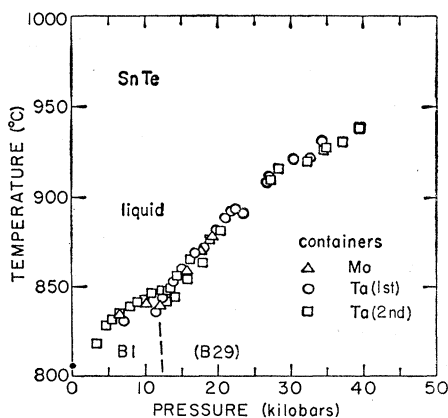


Fig. 1. Data on the melting of SnTe.

slope, but $\sim 5^\circ\text{C}/\text{kb}$ may be estimated.

Considerable curvature in the melting curve is evident (Fig. 1). There may be a maximum— $dT/dp = 0$ —near $\sim 11 \pm 1$ kb, although our experiments are not definitive. The upper limit to the difference in temperature between the possible maximum and the triple point is $\sim 4^\circ\text{C}$. If one takes the melting slope of the *BI* polymorph to be essentially zero at the triple point, thermodynamics requires that the volume decrease for freezing of the high-pressure polymorph equals that across the solid-solid transition. For the melting of the pressure-induced polymorph, dT/dp is $5.3^\circ \pm 1.0^\circ\text{C}/\text{kb}$ near the triple point and monotonically decreases to $2.4^\circ \pm 0.3^\circ\text{C}/\text{kb}$ near 40 kb. By uncertain extrapolation to higher pressures, a maximum in the melting curve might be possible above 60 or 70 kb. Extrapolation to lower pressures yields a metastable zero-pressure melting temperature of the denser polymorph at $750^\circ \pm 20^\circ\text{C}$.

Data for high-pressure phase transitions in the IV-VI compounds are limited. Volume measurements (8) suggest transitions for PbS near 24 kb and for PbSe and PbTe near 40 to 45 kb, with volume changes of 2 to 4 percent. Measurements of resistance at room temperature (9) under up to ~ 0.5 Mb corroborate the PbS transition but place near 75 to 80 kb the only transition found for PbTe; these transitions are characterized by large increases in resistance similar to that for the 18 kb SnTe transition (6). Ball's investigations (10) for PbTe place a solid-solid transition near 55 kb at room temperature and suggest a melting-curve maximum in the 20 to 40 kb range (11). The melting-curve maxima for SnTe and PbTe suggest highly compressible liquids related to group VI elements (for exam-

ple, 5). Although probably less common, there are liquids based on the group VI elements (such as CdTe and HgTe, 12) that must be relatively incompressible—as is indicated by the minimal curvature in the melting curves.

At zero pressure, PbS, PbSe, and PbTe possess the *BI* structure; nothing is reported of structures of the high-pressure polymorphs. For SnS, SnSe, GeS, and GeSe, the structure at zero pressure is *B29*. For GeTe, a rhombohedral distortion of the *BI* structure transforms (apparently continuously) to the *BI* structure at high temperatures; the transition temperature probably decreases with increasing pressure (13). Disordered analogs of these IV-VI structures are: *BI* \leftrightarrow simple cubic (sc); *B29* \leftrightarrow black phosphorus; rhombohedral GeTe \leftrightarrow *A7* (arsenic). Increasing pressure favors the transitions black phosphorus \rightarrow *A7* \rightarrow sc for P (14) and *A7* \rightarrow sc for Sb (15), and one might expect a similar sequence (namely *B29* \rightarrow rhombohedral \rightarrow *BI*) for the IV-VI compounds.

Identification by Kafalas and Mariano (6) of the high-pressure *B29* structure of SnTe is a significant departure from the simple sequence outlined above. Present inadequacies of x-ray diffraction at high pressure preclude definitive determinations of complex structures, especially those with positional parameters, although the indexing (6) for SnTe cannot be directly challenged now (16). The reported volume change (*BI* \rightarrow *B29*) of 7 percent (6) for SnTe appears to be much too large. Approximation of the volume change, on melting, of the high-pressure polymorph by this value of the solid-solid volume-change leads to an estimate of ~ 12 calories per formula weight \cdot degree for the entropy of fusion of the pressure-induced polymorph—much greater than the value of 6.55 for SnSe (17). The observed sequences (1) of pressure-induced polymorphs largely depend upon increases in coordination, and, for suitable values of the positional parameters, coordination can be greater in the *B29* than in the *BI* structure.

In cognizance of these difficulties, an empirical approach for comparison of densities of possible polymorphs is essayed for this family of compounds. As in a procedure recently devised by one of us (18), let a "characteristic dimension" be defined as the cube root of the volume per four formula units for each compound in each known struc-

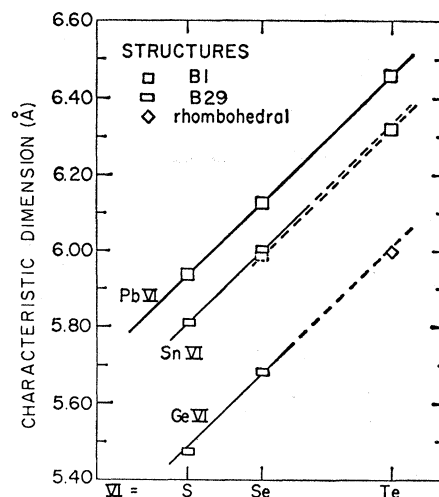


Fig. 2. Plot correlating "characteristic dimensions" (at zero pressure) for the various structures of the IV-VI compounds. The heavy line is arbitrarily assumed (see text).

ture. As in Fig. 2, plot the data (19) for an isostructural sequence (PbS, PbSe, PbTe) on an arbitrary straight line, with the characteristic dimensions as ordinates; the abscissas are now determined for the other IVS, IVSe, and IVTe compounds. Lines, parallel with the initial arbitrary line (the heavy line in Fig. 2) through the other isostructural sequences, are constructed; as Fig. 2 shows, the lines satisfactorily pass through the SnVI and GeVI data (*B29* structure). By extrapolation (of unknown validity), the *B29* structure seems to be slightly less dense than the *BI* structure for SnTe.

WILLIAM KLEMENT, JR.*

LEWIS H. COHEN

Department of Physics, University of California, Berkeley 94720, and Department of Geological Sciences, University of California, Riverside

References and Notes

- W. Klement and A. Jayaraman, *Progr. Solid State Chem.*, in press.
- L. H. Cohen, W. Klement, G. C. Kennedy, *J. Phys. Chem. Solids* **27**, 179 (1966).
- We thank R. L. Orr for the sample and its analysis.
- L. H. Cohen, W. Klement, G. C. Kennedy, *Phys. Rev.* **145**, 519 (1966).
- W. Klement, L. H. Cohen, G. C. Kennedy, *J. Phys. Chem. Solids* **27**, 171 (1966).
- J. A. Kafalas and A. N. Mariano, *Science* **143**, 952 (1964).
- R. F. Brebrick, *J. Phys. Chem. Solids* **24**, 27 (1963).
- P. W. Bridgman, *Phys. Rev.* **57**, 237 (1940); *Proc. Amer. Acad. Arts Sci.* **74**, 21 (1940); **76**, 55 (1948).
- G. A. Samara and H. G. Drickamer, *J. Chem. Phys.* **37**, 1159 (1962); A. A. Semerchan, L. F. Vereshchagin, N. N. Kuzin, L. N. Drozdova, *Soviet Phys. "Doklady" English Transl.* **8**, 586 (1963); A. A. Semerchan, N. N. Kuzin, L. N. Drozdova, L. F. Vereshchagin, *ibid.*, p. 982 (1964).
- D. L. Ball, in *Liquids: Structure, Properties, Solid Interactions*, T. J. Hughel, Ed. (Elsevier, New York, 1965), pp. 353-69; *J. Chem. Eng. Data* **10**, 37 (1965).

11. Runs with PbTe (3), sealed with Pyrex in Nb and Ta capsules (chromel-alumel and platinum-II thermocouples, respectively), were made in the range 6 to 38 kb. A rather flat maximum was suggested near $981^\circ \pm 3^\circ\text{C}$ and 25 to 33 kb.
12. A. Jayaraman, W. Klement, G. C. Kennedy, *Phys. Rev.* **130**, 2277 (1963).
13. K. Schubert and H. Fricke, *Z. Metallk.* **44**, 457 (1953).
14. J. C. Jamieson, *Science* **139**, 1291 (1963).
15. S. S. Kabalkina and V. P. Mylov, *Soviet Phys. "Doklady" English Transl.* **8**, 917 (1964); L. F. Vereshchagin and S. S. Kabalkina, *Soviet Phys. JETP English Transl.* **20**, 274 (1965).
16. We thank Q. Johnson for comments regarding the vagaries of high-pressure x-ray diffraction.
17. R. L. Orr and A. U. Christensen, *J. Phys. Chem.* **62**, 124 (1958).
18. A. Jayaraman, T. R. Anantharaman, W. Klement, *J. Phys. Chem. Solids*, in press.
19. (GeS) W. H. Zachariasen, *Phys. Rev.* **40**, 917 (1932); (GeSe) S. N. Dutta and G. A. Jeffrey, *Inorg. Chem.* **4**, 1363 (1965); (GeTe) J. Goldak, C. S. Barrett, D. Innes, W. Youdelis, *J. Chem. Phys.* **44**, 3323 (1966); (SnS) W. Hofmann, *Z. Krist.* **A92**, 161 (1935); (SnSe) B29, A. Okazaki and I. Ueda, *J. Phys. Soc. Japan* **11**, 470 (1956), B1 (i) obtained in vapor deposition by L. S. Palatnik and V. V. Levitin [*Dokl. Akad. Nauk SSSR* **96**, 975 (1954)] and (ii) consistent with extrapolations from SnSe-PbSe data of S. Yamamoto, *Sci. Rept. Tohoku Univ.* **40**, 11 (1956); PbS, PbSe, and PbTe are well known.
20. Supported by the Miller Institute (W.K.) and the Committee on Research (L.H.C.), University of California, Berkeley. We thank G. C. Kennedy for lending equipment.

* Present address: Department of Engineering, University of California, Los Angeles 90024.

4 August 1966

Mars Ice Caps

Abstract. *Minimum atmospheric temperatures required to prevent CO₂ condensation in the Mars polar caps are higher than those obtained in a computer experiment to simulate the general circulation of the Mars atmosphere. This observation supports the view that the polar caps are predominantly solid CO₂. However, thin clouds of H₂O ice could substantially reduce the surface condensation rate.*

Leighton and Murray (1) have argued that, in light of the new data on the surface pressure of Mars (2), the polar caps are most probably composed of solid CO₂ rather than of water ice, as previously supposed (3). They explicitly neglected the exchange of heat between the atmosphere and the ground, as well as the role of horizontal heat transfer by the atmosphere. These factors are considered here for two plausible models of atmospheric conditions over the Mars ice caps. The results tend to support the conclusions of Leighton and Murray, but downward emission by possible clouds of water ice introduces some uncertainties.

During the period of polar winter darkness, both solar radiation and heat

conduction in the ground can be ignored, and the heat balance condition at the ground surface is

$$\epsilon \sigma T_a^4 + H = \sigma T_g^4$$

where T_a is the atmospheric temperature (for simplicity the atmosphere is assumed to be isothermal), T_g is the ground surface temperature, ϵ is the atmospheric emissivity, σ is Stefan's constant, and H is the turbulent transfer of heat from the atmosphere to the ground. When the sense of H is to transfer heat downward, then the temperature gradient near the ground surface is stable, and we can use the bulk transfer law for H (4),

$$H = \rho C_p C_D |\mathbf{v}| (T_a - T_g)$$

where ρ and C_p are the surface air density and constant pressure specific heat, respectively, $|\mathbf{v}|$ is the surface wind speed, and C_D is the surface drag coefficient. Under terrestrial conditions over new snow or ice surfaces $C_D \approx .001$ (4).

The condition that no solid CO₂ be deposited on the ground is therefore that

$$\epsilon \sigma T_a^4 + \rho C_p C_D |\mathbf{v}| (T_a - T_g) \geq \sigma T_c^4$$

where T_c is the CO₂ condensation temperature (146.3°K for a 5 mb, 100 percent CO₂ atmosphere), for if this condition is not satisfied at any time, the ground will cool either to T_c or to some higher temperature at which the condition is satisfied. The right-hand side of this expression has been evaluated under two assumptions for ϵ for various values of $|\mathbf{v}|$, assuming that the atmosphere is composed almost entirely of CO₂ having a surface pressure of 5 mb.

In the first model ϵ is due only to carbon dioxide and water vapor, with the total amount of water vapor in an atmospheric column equal to 10⁻³ g/cm² consistent with observations (5). Under these conditions ϵ is a weak function of temperature, varying between 0.13 and 0.19 over the range 150° to 250°K.

In the second model ϵ is due to a cloud of ice crystals whose total column mass is 10⁻³ g/cm². This is about the densest cloud one might expect consistent with observations (5). Under the conditions of water vapor pressure and temperature on Mars one would expect ice particle sizes between those in terrestrial mother-of-pearl clouds and noctilucent clouds, that is, particles having a radius of 1 μ or less (6). Since, at the temperatures of interest,

the blackbody function peaks near 20 μ, the size parameter $\alpha \equiv 2\pi r/\lambda$ (r is the particle radius, λ the wavelength) is small enough that the absorption cross section can be approximated by

$$\sigma_a \approx -4\pi r^2 \alpha \cdot \text{Im} \left(\frac{m^2 - 1}{m^2 + 2} \right)$$

where m is the complex index of refraction (7). Under these conditions, the optical depth of the ice cloud depends only on the total ice content and is independent of the particle size; furthermore, scattering is quite negligible. If we use Kislovskii's data for m (8) and the above relation, $\epsilon = 0.73$ for the 10⁻³ g/cm³ cloud, and it is sensibly independent of temperature. Since the cloud is nearly black in the spectral region of CO₂ emission, inclusion of CO₂ emission at temperature T_a leads to practically the same emissivity.

The atmospheric temperatures required to prevent CO₂ deposition as a function of surface wind speed are shown in the figure for these two models. In the case of the clear sky, the combination of atmospheric temperatures and wind speeds required seems far too high to prevent CO₂ deposition, especially in view of the fact that higher air temperatures over the polar region reduce the horizontal temperature gradient and consequently reduce the horizontal heat flux into the polar region. In the case of the ice cloud, it is not certain that the required temperatures are too high. However, a numerical experiment to simulate the the circulation of the Mars atmosphere has recently been carried out, the primitive equations of atmospheric motion

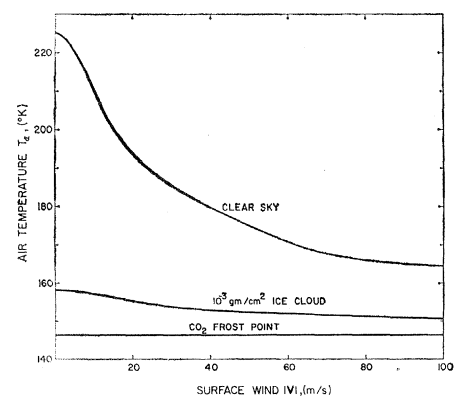


Fig. 1. Minimum temperatures of an isothermal CO₂ atmosphere required to prevent CO₂ frost formation for a 5 mb surface pressure. The figure can be interpreted for values of the drag coefficient other than .001 by identifying the abscissa scale with $(10^8 C_D |\mathbf{v}|)$ rather than with $|\mathbf{v}|$.